

Supporting Information

Surface residence and uptake of methyl chloride and methyl alcohol at the air/water interface studied by vibrational sum frequency spectroscopy and molecular dynamics

Kandice Harper, Babak Minofar,[‡] M. Roxana Sierra-Hernández, Nadia N. Casillas-Ituarte, Martina Roeselova,^{‡*} Heather C. Allen*

*Department of Chemistry, The Ohio State University, 100 West 18th Ave., Columbus, OH 43210 and
[‡]Institute of Organic Chemistry and Biochemistry, Academy of Sciences of the Czech Republic, Flemingovo nam. 2, 16610 Prague 6, Czech Republic.

SFG polarization studies

PPP and SPS polarization combination spectra were obtained and are shown in Figures S1 and S2, respectively.

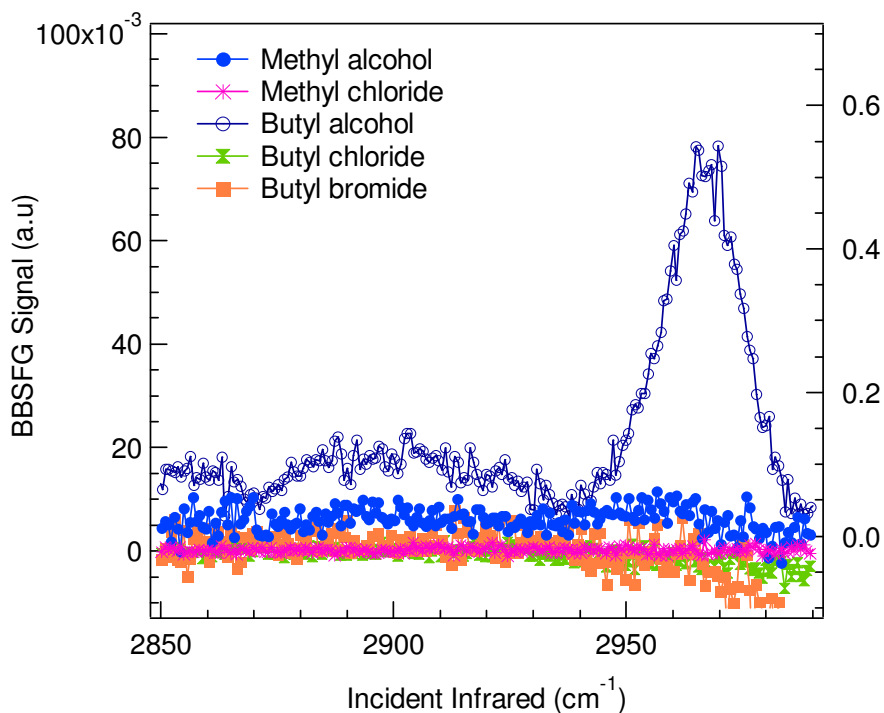


Figure S1. VSGF PPP spectra from flow experiments over water of methyl alcohol, methyl chloride, butyl alcohol, butyl chloride, and butyl bromide. The left axis is used for the butyl halides.

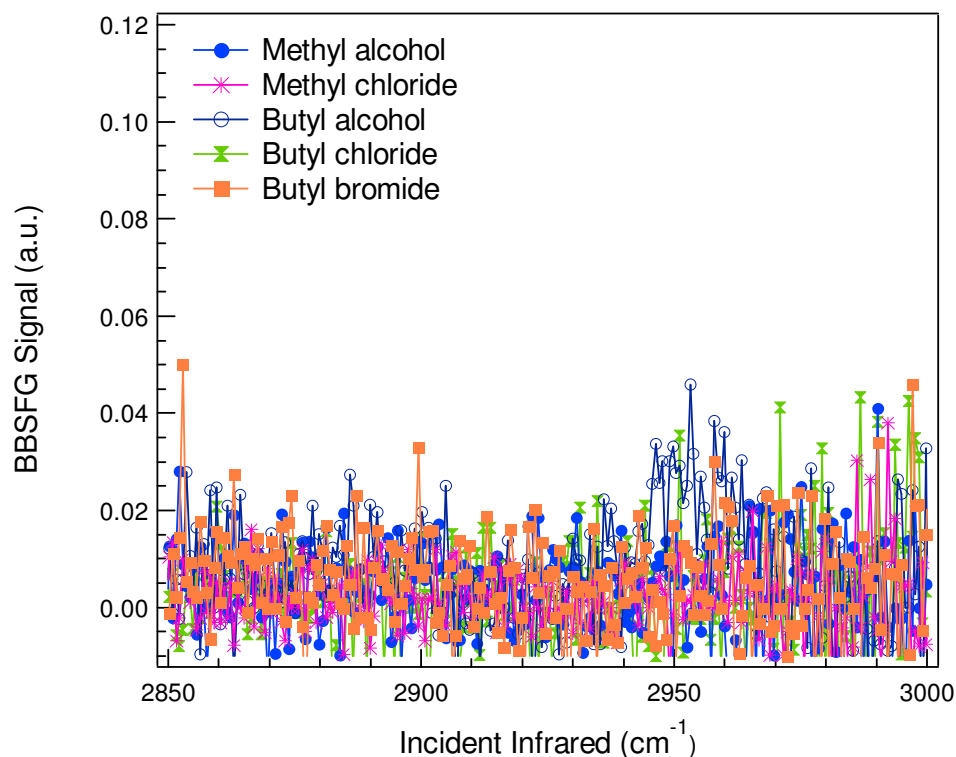


Figure S2. VSFG SPS spectra from flow experiments over water of methyl alcohol, methyl chloride, butyl alcohol, butyl chloride, and butyl bromide.

Gas-phase Concentrations

The gas phase concentration of CH_3OH and CH_3Cl was determined by using a Thermo Nicolet FTIR spectrometer (Avatar 370, Thermo Electron Corporation). A mixture of $\text{N}_2/\text{CH}_3\text{OH}$ was flowed at 15 standard cubic centimeters per minute (sccm) over 24 mL of water in a Petri dish contained in the flow chamber placed in the FTIR sample compartment, whereas CH_3Cl was flowed at 10 sccm. The flow conditions for each compound were kept the same as described for the surface analyses completed by the broad bandwidth sum frequency generation (BBSFG). Continuous IR spectra (50 scans, 4 cm^{-1} resolution) were obtained for up to two hours. The concentration of CH_3OH was determined by using the absorbance of the $\nu_{\text{CO-ss}}$ at 1052 cm^{-1} and the cross section reported on HITRAN data base ($1.388 \times$

$10^{-20} \text{ cm}^2/\text{molecule}$).¹ The concentration of CH_3Cl was estimated by using the absorbance of the $\nu_{\text{CH}_3-\text{SS}}$ at 2922 cm^{-1} .¹ The CH_3OH and CH_3Cl concentrations are shown in Figure S3. The CH_3OH and CH_3Cl concentrations after two hours were determined to be 4.16×10^{17} and 1.17×10^{19} molecules/ cm^3 , respectively. These results show that CH_3Cl gas phase concentration was two orders of magnitude greater than that of CH_3OH , and therefore the gas phase concentration was not a limiting condition for the lack of SFG signal of CH_3Cl .

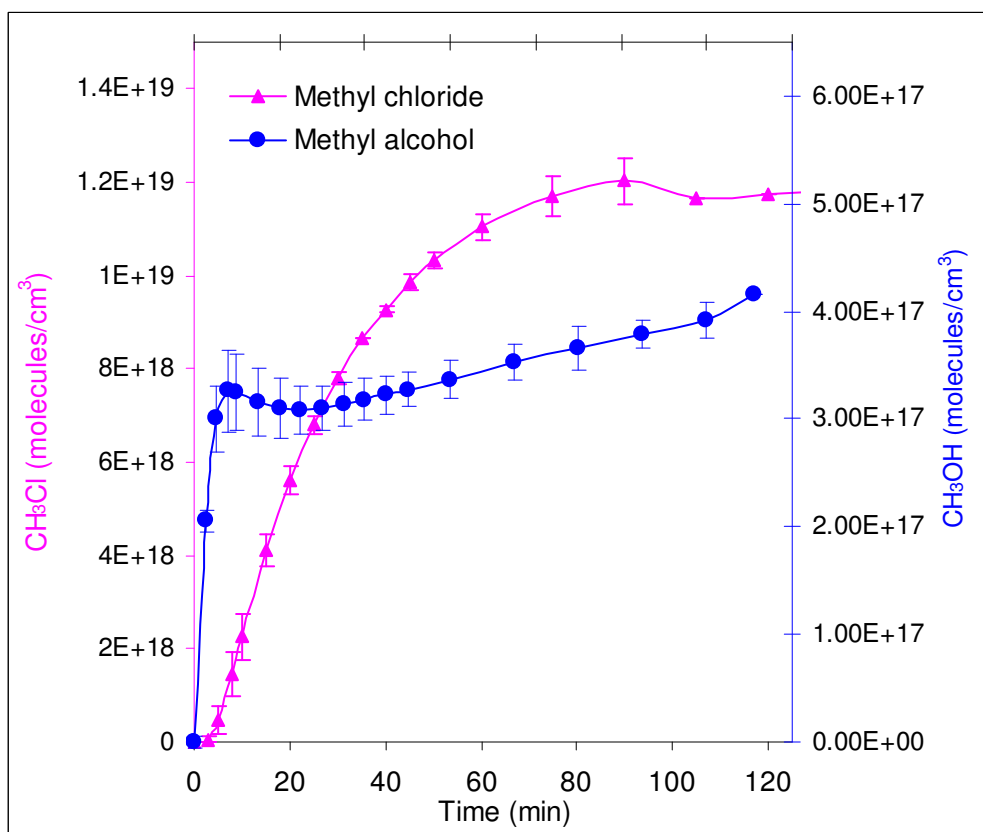


Figure S3. Gas phase concentration of CH_3Cl and CH_3OH over time.

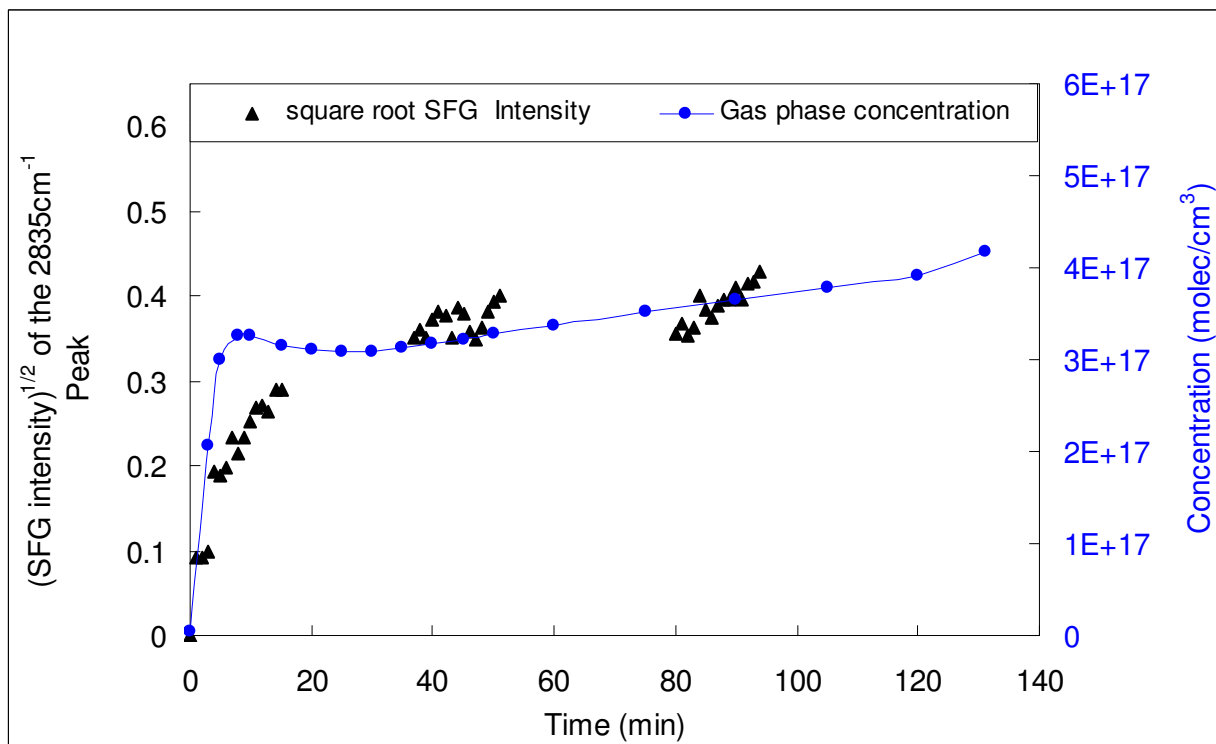


Figure S4. Gas phase concentration of CH₃OH over time compared against the square root of the VSFG intensity (2835 cm⁻¹ peak).

Bulk Concentrations

A CH₃OH calibration curve was developed from FTIR spectra by integrating the peaks at 1052 cm⁻¹ to determine the bulk concentration in the flow experiments and is shown in Figure S5. The concentration of CH₃OH in aqueous solution followed a linear trend for up to 2h. The solution concentrations of CH₃OH were determined at 30, 60 and 120 minutes of flow from the calibration curve. Three concentrations are shown in Table S1.

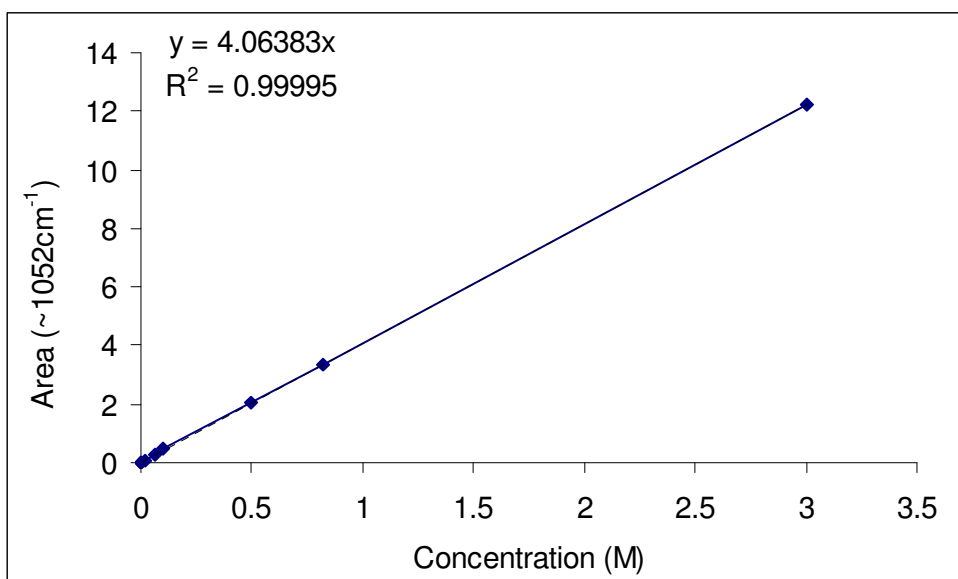


Figure S5. Calibration curve of bulk CH₃OH.

Table S1. CH₃OH bulk concentration of flow experiments.

Time (min)	Concentration (M)	St. dev
30	0.110	0.007
60	0.19	0.016
120	0.45	0.014

For all CH₃OH flow experiments, the glass vial containing the CH₃OH was weighed before and after the flow. The weight difference was used to calculate the total number of molecules flowed into the chamber and is shown in Table S2 (second column). During the flow, molecules diffuse into the 24 mL of water (number calculated from the calibration curve, third column), while others stay in the gas phase (measured by FTIR, fourth column).

Table S2. Number of CH₃OH molecules total (calculated by weight loss), in aqueous phase, and in gas phase.

Time (min)	Total number of molecules	Molecules in 24 mL water	Molecules in gas phase
30	2.06×10^{21}	1.71×10^{21}	3.10×10^{17}
60	5.21×10^{21}	3.01×10^{21}	3.37×10^{17}
120	9.12×10^{21}	6.43×10^{21}	3.92×10^{17}

The number of molecules in water added to the number of molecules in the gas phase after 30 min of flow was 1.79×10^{21} molecules/cm³, which is ~ 85% of the number of molecules calculated by weight loss. The summation of the number of molecules in the condensed and gas phase after 60 and 120 min of flow are 3.10×10^{21} and 6.53×10^{21} molecules/cm³ respectively. These two values are ~ 60 % and 70% from those calculated by weight loss, suggesting that water surface is becoming saturated by CH₃OH molecules.

Evaluation of the infrared energy

The SFG intensity is proportional to the intensity of both the visible and infrared beams as shown in the equation below.

$$I^{\omega_{SFG}}(\omega) \propto \left| E^{\omega_{SFG}} \cdot \chi^{(2)} : E^{\omega_{VIS}} E^{\omega_{IR}} \right|^2 I^{\omega_{VIS}} I^{\omega_{IR}}$$

$I^{\omega_{SFG}}$, $I^{\omega_{vis}}$, and $I^{\omega_{IR}}$ are the intensities of the sum frequency, incident visible, and incident infrared beams, respectively. Therefore, if the infrared beam is completely absorbed by gas phase molecules before reaching the interface there will not be generation of the sum frequency photons. To verify that there were sufficient infrared photons after flowing alkyl halides, the infrared energy coming out of the chamber was measured. This set of experiments was performed on a scanning SFG (SSFG) system. Details of the SSFG system can be found in previous publications.² The infrared beam reflected from a gold mirror was monitored as the infrared beam was scanned from 2800 to 3100 cm^{-1} . A scan of the empty chamber was acquired and is shown in Figure S6 (initial). There is a relative constant infrared energy of $\sim 180 \mu\text{J}$ in this wavenumber range. Then a mixture of N_2 /methyl alcohol (CH_3OH) gases was allowed to enter the chamber with a flow rate of 15 sccm as described in the Experimental Section of the manuscript. After approximately an hour of flow the infrared energy was measured from 2800 to 3100 cm^{-1} (Figure S6). The chamber was then evacuated with pure N_2 until the initial infrared energy ($\sim 180 \mu\text{J}$) was recovered. Then methyl chloride (CH_3Cl) was flowed at 10 sccm into the chamber. The infrared energy after ~ 40 min of flow was measured and is also shown in Figure S6. Several dips are observed in the CH_3OH and CH_3Cl spectra. These dips correspond to the absorbances (assigned to CH_3 symmetric stretch and CH_3 Fermi resonance) of the gas phase molecules of CH_3OH and CH_3Cl . Also, it was observed that the infrared energy after CH_3OH flow was always lower than that observed after CH_3Cl flow. From these results, it can be suggested that the infrared energy after CH_3Cl flow was sufficient to generate sum frequency signal. The same procedure was followed for the measurement of the infrared energies after the flow of butyl alcohol and butyl halides (data not shown). The flow conditions were kept the same as described for the surface analysis. In all cases, the resultant infrared energy of the alcohols was lower than that observed for the alkyl halides. This data was reproduced by infrared measurements from Fourier transform infrared (FTIR) spectroscopy using similar flow conditions as described below in the concentration measurements.

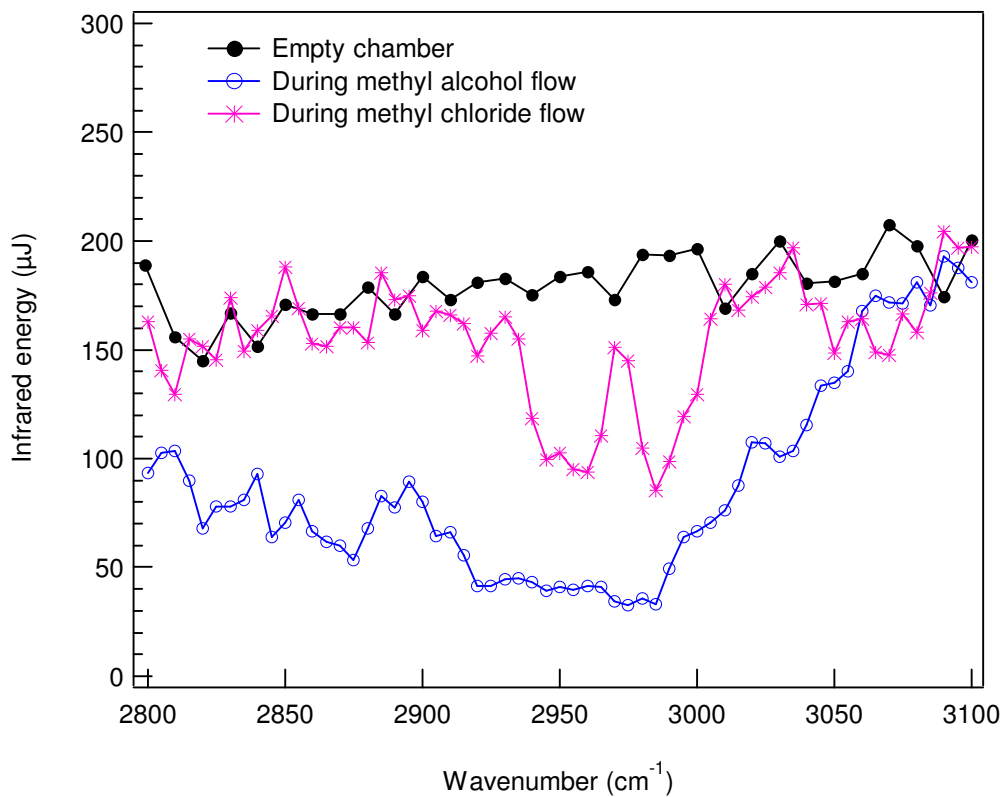


Figure S6. Infrared energy versus wavenumber at initial conditions (empty chamber) and during the flow of CH_3OH and CH_3Cl .

Raman studies of the bulk solutions

Raman spectra of the aqueous solutions after the flow of the (a) methyl and (b) butyl species were obtained and are shown in Figure S7. Note: the spectral region between 600 to 1100 cm^{-1} was also acquired to look for the C-Cl and C-Br stretches for the butyl species (spectra not shown), but no peaks were detected. Spectra show that methyl species and butyl alcohol are adsorbed into the bulk phase.

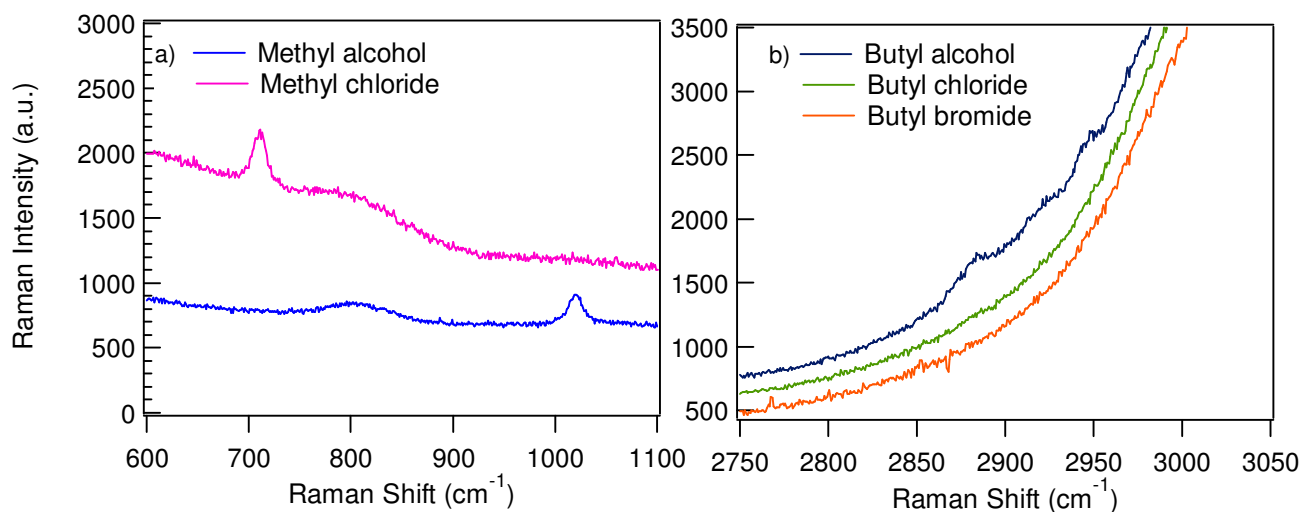


Figure S7. Raman spectra of the aqueous solutions after the flow of the (a) methyl and (b) butyl species.

References

- (1) Rothman, L. S.; Jacquemart, D.; Barbe, A. C. B., D.; Birk, M.; Brown, M. R.; Carleerf, L. R.; Chackerian Jr, C.; Chance, K.; Coudert, L. H.; Dana, V.; Devi, V. M.; Flaud, J.-M.; Gamache, R. R.; Goldman, A.; Hartmann, J.-M.; Jucks, K. W.; Maki, A. G.; Mandin, J.-Y.; Massie, S. T.; Orphal, J.; Perrin, A.; Rinsland, C. P.; Smith, M. A. H.; Tennyson, J.; Tolchenov, R. N.; Toth, R. A.; Vander Auwera, J.; Varanasiq, P.; Wagner, G. *Journal of Quantitative Spectroscopy & Radiative Transfer* **2005**, *96*, 139-204.
- (2) Liu, D.; Ma, G.; Xu, M.; Allen, H. C. *Environ. Sci. Technol.* **2005**, *39*, 206-212.